Identification of the Friction Potential for the Application in an Automated Emergency Braking System

Dipl.-Ing. Cornelia Lex*
Dr. Hans-Ulrich Kobialka**
Dr. Arno Eichberger*

* *Graz University of Technology, Institute of Automotive Engineering, Graz, Austria*
** *Fraunhofer Institute for Intelligent Analysis and Information Systems (IAIS), St. Augustin, Germany*

Abstract

The capabilities of Automated Emergency Braking Systems (AEB) can be significantly improved when the actual friction between tires and road is known. In this work, it is investigated whether an estimation of the friction potential based on sensor data is feasible with an accuracy sufficient for an AEB. Recurrent neural networks trained by Echo State Networks (ESNs) are used to estimate friction potential from sensor data. Measurements have been conducted on a proving ground with three different tire types, two different surfaces, different driving manoeuvres and different tire inflation pressures. Standard on-board sensors of the vehicle and advanced measurement equipment have been used to measure the vehicle reaction. Based on this work, a a rough understanding is gained on how well the friction potential can be estimated in certain situations.

1. Introduction

Automated Emergency Braking systems (AEB) will become a standard part of commercial vehicles and passenger cars within the next years. According to EU directive 347/2012, fitment of AEB will be required for commercial vehicles above 3.5t beginning from the 1st of November 2013 for new type approvals, and from the 1st of November 2015 for all new vehicles. Beginning in 2014, EURO-NCAP will take into account in the star rating whether AEB is implemented in passenger vehicles, and, for 2016, also whether AEB are enhanced by a pedestrian detection.

Traffic research showed that a high number of rear-end crashes happens because drivers do not brake hard enough, react too late or fail to react because they are distracted, (Breuer 2009). AEB intervene autonomously in order to assist drivers that fail to react or react too late. The importance of these systems is demonstrated in several studies dealing with the efficiency of driver assistance systems. Busch et al. reported benefit potentials for collision avoidance of 3% for conventional Brake Assist systems (BA), and 6% for AEB for all fatal accidents in Germany, see (Busch, Brunner et al. 2006). Eichberger et al. showed an estimation of potential of avoiding fatalities using AEB ranging in between 13% to 22%, depending on the intervention strategy and the reaction of the driver to collision warnings, (Eichberger, Tomasch et al. 2011).

However, current AEB systems are designed to meet requirements for collision avoidance and mitigation on dry roads. The maximum coefficient of friction between tires and road, further on referred to as friction potential μ_G, is an important parameter for a future improvement of AEB. On road surfaces with reduced friction potential e.g. due to bad road condition, the activation times will not be sufficient. But investigations suggest that collision avoidance systems have the highest benefit on low fric-

tion surfaces, e.g. (Niederkofler, Lex et al. 2011). Currently standardisation of testing procedures is in progress. However, standards will be proposed for dry roads.

2. Automated Emergency Braking System (AEB)

The type of AEB considered in the following consists of four phases. In the *first phase*, the so-called detection phase, a possible collision is identified. In the *second phase*, the driver is either warned by an acoustical, optical or haptic device. If the driver fails to react, the AEB starts its *third phase* with a partial-braking manoeuvre to reduce the vehicle speed. Still, the possibility for the driver to independently intervene, like steering around a possible obstacle, remains. In the *fourth phase*, full braking is started under the premise that the driver still has not reacted.
The rate of missed interventions has to be kept low, but false AEB interventions have to be avoided as the outcome can be very critical. False interventions in uncritical situations can provoke accidents like a rear crash. In case of doubt, an AEB intervention has to be omitted. In order to maximize the confidence in a detected collision, the activation of a phase is started at the latest possible time. Typically, collision warnings are issued 1.5 to 2.5 seconds, and (in case of no driver reaction) automated braking starts 0.6 an 1.0 seconds before collision.
The maximum achievable decelerations for partial and full braking and therefore the activation times depend on the friction potential μ_G. On surfaces with low friction potential, the activation of the different phases has to be done earlier in order to avoid a collision.

Requirements for accuracy of friction potential estimate

Considering a simplified braking manoeuvre based on (Mitschke, Wallentowitz 2004), the brake pedal is actuated at an initial speed $\boldsymbol{v_{x0}}$, see the continuous black line in figure 1. After the response time of the braking system where the vehicle's speed still remains constant, the braking pressure is build up linearly during the period $\boldsymbol{t_s}$. Then, full deceleration $\boldsymbol{\ddot{x}_{ref}}$ is available constantly until the vehicle stops after time $\boldsymbol{t_{ref}}$. For ideal braking conditions, the achievable accelerations result in $\boldsymbol{\ddot{x}_{ref} = -\mu_{ref} \cdot g}$, wherein $\boldsymbol{g}$ denominates the gravitational acceleration and $\boldsymbol{\mu_{ref}}$ the current friction potential. If the collision with a standstill object is avoided and the vehicle is at full stop, the impact speed $\boldsymbol{\Delta v}$ is zero:

$$\Delta v = v_{x0} + \frac{\ddot{x}_{ref}}{2} t_s + \ddot{x}_{ref} \cdot t_{ref} = v_{x0} - \frac{\mu_{ref} \cdot g}{2} t_s - \mu_{ref} \cdot g \cdot t_{ref} \stackrel{\text{def}}{=} 0. \qquad (1)$$

An estimate of the friction potential is not ideal, so inaccuracies $\boldsymbol{\Delta\mu}$ have to be taken into account. Then, the estimate can be written as $\boldsymbol{\hat{\mu} = \mu_{ref} \pm \Delta\mu}$. Also, a time delay

$\boldsymbol{t_M}$ until the estimate is available with sufficient accuracy has to be considered. Substituting $\hat{\boldsymbol{\mu}}$ for $\boldsymbol{\mu_{ref}}$ in equation (1) and assuming that the brake pedal is actuated after the time delay $\boldsymbol{t_M}$, the impact speed results in

$$\begin{aligned}\Delta v &= v_{x0} + \frac{-\hat{\mu}\cdot g}{2} t_s + (-\hat{\mu}\cdot g)\cdot\left(t_{ref} - t_M\right) \\ &= v_{x0} + \frac{-\hat{\mu}\cdot g}{2} t_s + (-\hat{\mu}\cdot g)\cdot\left(\frac{v_{x0}}{\mu_{ref}\cdot g} - \frac{t_s}{2} - t_M\right).\end{aligned} \tag{2}$$

A constant time delay t_M can be assumed. The relation for $\Delta\mu$ is given when rearranging equation (2) for $\Delta\mu$. Its dependence on μ_{ref} and v_{x0} can be seen in figure 2.

Underestimating μ_G results in a shorter braking distance than expected by the system. The collision is avoided, but valuable verification time for the collision prediction is lost in the decision phase of the AEB. The consequence is a higher risk for false interventions and the loss of driver acceptance. If the estimated μ_G is higher than the actual one, the collision cannot be avoided and the impact speed Δv is not zero. An acceptable impact speed is set using the RCAR low-speed structural crash test which is conducted with a Δv of 15 km/h, (Research Council for Automobile Repairs 2011). This procedure was implemented to assess the damageability and ability to repair vehicles after low-speed front collisions. Regarding the weakest traffic participants, namely pedestrians, this impact velocity is suitable in scenarios where an AEB would intervene. At an impact speed of 15 km/h, the probability for a pedestrian to die[1] in a car collision is 0.2% and the probability for severe injuries[2] is 3.1%, according to (Rosén, Sander 2009).

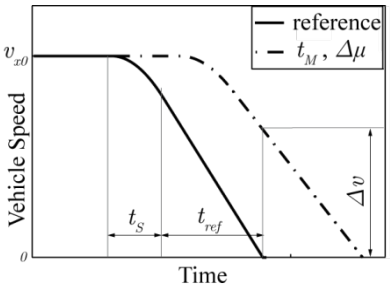

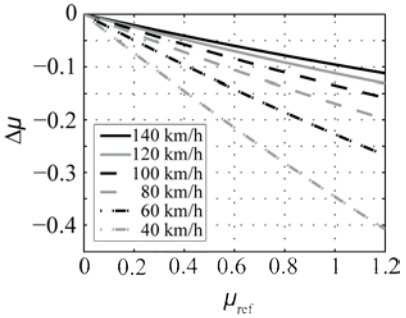

[1] corresponds to the injury criterion MAIS 5+
[2] corresponds to the injury criterion MAIS 3+

Figure 1 – Speed profile during braking manoeuvre to define requirements on estimate concerning time delay and accuracy

Figure 2 – Relation between acceptable accuracy $\Delta\mu$ and the real friction potential μ_{ref} for different initial speeds v_{x0} calculated for an impact speed Δv of 15 km/h and a time delay t_M of 0.05 s

3. Estimation of the Friction Potential Using Echo State Networks

Recurrent Neural Networks (RNNs) are artificial neural nets containing feedback loops, similar to biological neural networks like in the brain. In contrast to RNNs, so called Feed Forward Neural Networks (FFNN) do not contain any feedback loops, (Haykin 1999). Mathematically speaking, the fundamental difference between RNNs and FFNNs is that FFNN implement functions, while RNNs are dynamical systems, similar to systems described by differential equations.

Regarding time series analysis, time series data can be continuously fed into an RNN. Because of its feedback loops, previously received input signals are still represented in the net. This kind of memory enables an RNN to learn models of highly non-linear systems which then, in turn, can be used for simulation, pattern matching, classification, and prediction of time series.

So far, this potential could not be fully exploited because there were no simple methods to train RNNs in a stable way. Gradient-based methods e.g. back-propagation through time (BPTT), (Haykin 1999), were used, but these require a lot of experience which in turn limits the size of the used nets and the problems to be tackled.

Echo State Networks (ESNs) is a new approach of training RNNs, (Lukosevicius, Jaeger 2009). The advantage of ESNs is that only the connections to the output nodes are computed during training. This is done using regression which is far more simple and stable than compared to gradient-based methods. This enables the use of large nets having several thousand internal nodes. These large nets have the capacity of learning high-dimensional temporal patterns.

Echo State Networks are well recognized because of publications in well-known international journals like ‚Science' and ‚Neural Networks', see (Jaeger, Haas 2004) and (Jaeger, Maass W. et al. 2007).

In our experiments, we analysed whether it is possible to estimate the friction potential μ_G and the wheel-individual friction potenials $\mu_{R,i}$ (see *Determination of Reference Value*) during driving based on the data recorded by the mounted sensors. We

did this by training an Echo State Network (ESN) on measurement data and then evaluating the trained ESN on measurement data not used for training. The ESN was trained in a supervised way to learn the mapping from sensor data time series to friction potential time series, figure 3.

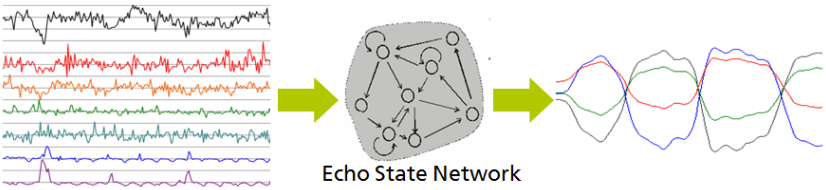

Figure 3 – Schematic Approach of Echo State Networks

Used Data

Measurements were conducted on Contidrom proving ground with an *Audi A4 Avant 1.8 TFSI* including several driving manoeuvres, see table 1. Three different tire types with different inflation pressures were evaluated on dry and wet road surfaces, see table 2 and table 3.

The wind velocities on the proving ground were $\leq$ 5.2 m/s during all measurements and the road surface temperature varied between 16.5 and 30 °C. Quasi-steady-state driving manoeuvres of at least 15 minutes were conducted before starting the measurements to ensure that the tires were at operating temperature. The inflation pressures were set at operating temperature of the tires. Altogether, 98 driving manoeuvres have been performed.

Table 1 - Performed Driving Manoeuvres

Sinus test according to (ISO 7401 2003)	Number of manoeuvres
Full and partial braking tests, Acceleration tests	41
Circuits on handling course I (dry asphalt)	11
Circuits on handling course II (wet asphalt)	5

Table 2 - Tire Types and Inflation Pressures

Summer tire, Dimension 245/40 R18	2.3 bar	13
	2.7 bar	12
	3.0 bar	10
Winter tire, Dimension 205/55 R16	2.3 bar	25
	3.0 bar	15
Slick tire, Dimension 245/64.5 R18	2.0 bar	12
	2.7 bar	11

Table 3 - Road Geometry and Surface Type

Straight course I, Asphalt dry	67
Straight course II, Asphalt wet	15
Handling course I, Asphalt dry	11
Handling course II, Asphalt wet	5

Both the standard on-board sensors of the vehicle as well as an advanced measurement equipment to evaluate the vehicle dynamics have been used.

The on-board vehicle sensors record the wheel speeds of all four wheels, the steering wheel angle, the vehicle's longitudinal velocity in the COG (centre of gravity), the engine's rotational speed, the engine torque, the accelerator pedal position, the vehicle's yaw rate and the environment temperature.

Information on the signals measured with the advanced vehicle dynamics measurement equipment is given in table 4. The sample frequency for all signals was 200 Hz.

Table 4 – Advanced Vehicle Dynamics Measurement Equipment (index $i = 1, \dots, 4$ denote the four wheels; index $k = 1,2$ denote the front wheels)

Signal	**Sensor**	**Unit**	**Accuracy**
Spring deflections s_i	-	mm	$< \pm 0{,}5\%$ FSO[4] (625mm)
Braking pressure for 2 brake circuits	-	bar	$< \pm 0{,}5\%$ FSO[4] (350 bar)
Wheel Camber angles γ_k	DCA	°	$< \pm 0.5°$
Wheel Velocities[3] v_k	SFII	m/s	$< \pm 0.5\%$ FSO[4] (250 km/h)
Wheel Slip Angle α_k	SFII	°	$< \pm 0{,}5°$
Chassis Velocities3	SHR	m/s	$< \pm 0.2\%$ FSO4 (250 km/h)
Chassis Side-Slip Angle	SHR	°	$< \pm 0{,}1°$

[3] Absolute value as well as longitudinal and lateral components
[4] Full Scale Output

Chassis Accelerations[5] in COG	ADMA	mG	< 1 mG
Chassis Rotational Velocities5	ADMA	°/s	$< 0{,}00004$ °/s

Determination of Reference Values

For each combination of road surface and mounted tire, a global friction potential μ_G has been identified based on driving manoeuvres near the limits of the maximum achievable accelerations. To ensure that the driving manoeuvres were at the limits, the slip angles at the maximum lateral acceleration $a_{M,y}$ were compared to lateral tire characteristics measured on a test bench. Based on a simplified vehicle model, the following relationship between the friction potential $\mu_{G,y}$ in lateral direction and $a_{M,y}$ is assumed:

$$\mu_{G,y} = \frac{a_{M,y}}{g}. \tag{1}$$

Longitudinal tire characteristics were not available, so the identified friction potential is only based on the measured accelerations achieved during braking. Usually, the longitudinal potential of tires is higher, but the comparison between the achieved longitudinal and the lateral accelerations showed similar results. So it was further on assumed that the friction potential was the same in longitudinal and lateral direction:

$$\mu_{G,x} \approx \mu_{G,y} \approx \mu_G. \tag{2}$$

In addition to the global friction potential μ_G, also wheel-individual friction potentials $\mu_{R,i}$ are estimated, see equation (3). They indicate the maximum transmittable forces on each tire and can be used to enhance the AEB strategy.

$$\mu_{R,i} = \mu_G \cdot \mu_{meas}(F_{z,i}(t)). \tag{3}$$

The value μ_{meas} is a function of the time variant dynamical vertical force $F_{z,i}$ acting on each tire i and is determined based on the lateral tire characteristics measured on a tire test bench. The dynamical vertical forces $F_{z,i}$ were calculated using a two-track vehicle model validated using measurements.

4. Data Analysis and Results

It was investigated how the reference values (described in the previous section) can be estimated based on the sensor data. We did this analysis using Echo State Networks.

The recorded measurements have different lengths in time ranging from 5 up to 630 seconds. Unfortunately the optical speed sensor measuring at the left wheel got bro-

[5] Longitudinal, lateral and vertical according to (DIN 70000 1994)

ken early during the manoeuvres, and the corresponding ones at the right wheel were heavily distorted when driving on wet road.

In a first series of experiments, we only used measurements on dry roads in order to exploit the data recorded from the optical speed sensor at the right wheel.

We further separated the data into four sets: three sets each containing only measurements using a particular tire (summer, slick, or winter tire) and one set containing data of all three tires. We then performed Leave-one-out cross-validation (LOOCV) for all these four sets.

Table 5 – The mean absolute error for ESNs trained on four different data sets

	LOOCV on Summer Tires	LOOCV on Slick Tires	LOOCV on Winter Tires	LOOCV on all tires
$\Delta\mu_{R,1}$	0.0016	0.0033	0.0012	0.0453
$\Delta\mu_{R,2}$	0.0016	0.0030	0.0013	0.0466
$\Delta\mu_{R,3}$	0.0009	0.0018	0.0008	0.0469
$\Delta\mu_{R,4}$	0.0010	0.0021	0.0007	0.0503
$\Delta\mu_{G}$	0.0	0.0	0.0	0.0483

For LOOCV on summer tire data, learning the global friction potential μ_G was trivial, because it was the same for all measurements. Also, the estimation of the wheel-individual friction potentials $\mu_{R,i}$ worked very well. The same holds true for LOOCV on slick and winter tire data.

LOOCV on data obtained with different tires is more challenging, because the global friction potential μ_G varied within the data set. Estimation of μ_G turned out to be the main challenge.

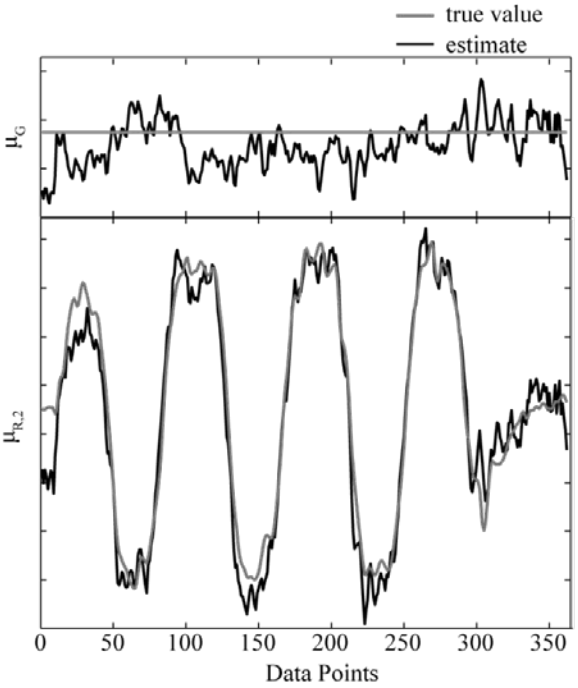

Figure 4 – Example of good estimation of $\boldsymbol{\mu_G}$ (black line, above) that also leads to good estimation of $\boldsymbol{\mu_{R,1}}$ (black line). The true values for $\boldsymbol{\mu_G}$ and $\boldsymbol{\mu_{R,1}}$ are plotted grey lines, respectively.

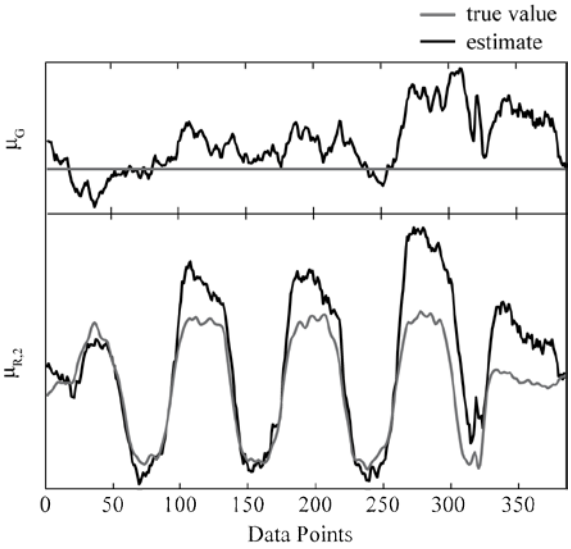

Figure 5 – In this example, estimation of $\boldsymbol{\mu_G}$ (black line, above) gets worse between time step 250 and370. Accordingly, estimation of $\boldsymbol{\mu_{R,2}}$ (black line) deviates from the true values for $\boldsymbol{\mu_{R,2}}$ (grey line) too

In cases when the estimation of μ_G was good, the estimation of $\mu_{R,i}$ also went well (see figure 4 and 5). If μ_G was badly estimated, this was also the case for $\mu_{R,i}$. These results are in accordance to the computation of $\mu_{R,i}$, see equation (3). From this we conclude that the ESN can (implicitly) estimate $\mu_{meas}(F_{z,i}(t))$ quite well.

In a second experiment, we used all measurement data obtained both on dry and wet roads, see table 6. We had to neglect the measurements of the optical sensor because (as mentioned above) they were distorted on wet road. On the positive side, we now had (compared to the experiments above) more measurements covering more road conditions and driving situations.

Table 6 - The mean LOOCV absolute error for the ESNs trained on all manoeuvres on both dry and wet roads.

	LOOCV on all manoeuvres with all tires on both dry and wet roads	LOOCV on all manoeuvres with Winter tires on both dry and wet roads

$\Delta\mu_{R,1}$	0.0532	0.0279
$\Delta\mu_{R,2}$	0.0530	0.0282
$\Delta\mu_{R,3}$	0.0545	0.0282
$\Delta\mu_{R,4}$	0.0571	0.0287
$\Delta\mu_{G}$	0.0569	0.0383

Estimation of μ_G is influenced by the road condition and the tire used. While the road condition may change dynamically, the tire of a vehicle does not during one trip. In the next consideration known tires are assumed which eases the estimation task. In an experiment, we trained an ESN model only on manoeuvres where winter tires were used. This means that the ESN model "assumes" that only winter tires are used. The LOOCV result in table 6 confirms that for known tires, the results get significantly better.

During the experiments, it turned out that the estimation of μ_G was very bad, once certain measurement time series were included into the training data. Investigations revealed that the true reference values for μ_G were incorrectly computed for some cases. So the ESN was very useful to detect such kind of inconsistencies in the data set.

We then visually inspected the parts of measurement time series, where ESN results showed significant deviations.

Firstly we identified situations where sensor values were distorted or did not work properly. This data was excluded in order to obtain a consistent data set. If these sensors are used later on the vehicle during real time operation, 'watch dog' software has to ensure that only non-distorted sensor data is fed into the ESN. Note that this was done for a few exceptional cases. ESN showed good estimations on quite noisy sensor data. And of course this data remains in the training set in order to make μ_G estimation robust with respect to sensor noise encountered during normal operation.

Secondly, we identified situations where sensors are not able to estimate μ_G properly. This happened mostly when the vehicle is not exposed to any acceleration. On the contrary, estimation of μ_G worked very well during acceleration and cornering, in particular for sinus driving.

5. Discussion

For the analysed manoeuvre data, the ESN method worked very well for μ_G estimation. It helped to detect inconsistencies and severely distorted sensor data. The remaining deviations turned out to be because μ_G can't be estimated in such situations, at least with the sensory equipment used.

The achievable accuracy was acceptable for different combinations of the initial speed v_{x0} and the friction potential μ_{ref}, compare table 6 and figure 2. For example, for inner-city speeds of about 60 km/h, a $\Delta\mu_G$ of 0.0569 (LOOCV of all tires, all manoeuvres and all road conditions, see table 6) is sufficient for friction potentials $\mu_{ref} \geq 0.23$. For highway speeds of about 140 km/h, the accuracy is sufficient for $\mu_{ref} \geq 0.57$.

For a known tire, the accuracy of the estimate is significantly higher. The following results are calculated for winter tires with a $\Delta\mu_G$ of 0.0383 (LOOCV of winter tires, all manoeuvres and all road conditions, see table 6). For an initial speed of 60 km/h, the estimate is sufficient for $\mu_{ref} \geq 0.16$ and for 140 km/h for $\mu_{ref} \geq 0.37$. Regarding further applications, this implies that knowledge of the mounted tire will be very helpful in order to achieve acceptable accuracies.

The experiences with the estimation of μ_G and $\mu_{R,i}$ showed, that implicitly $\mu_{meas}(F_{z,i}(t))$ and therefore $F_{z,i}(t)$ can be estimated quite well. Estimates of $F_{z,i}(t)$ might be used for certain vehicle dynamics controls or advanced driver assistance systems.

A question not investigated yet is to find a minimal set of sensors. Of course, sensors are expensive, but in addition they may also fail. In such a case, μ_G estimation and therefore AEB may fail too. In the future we will investigate minimal sensor configurations.

We will conduct further driving trials to cover a broader spectrum of driving situations. In particular we will investigate how quick a change of road conditions can be detected.

6. Conclusions

The activation times of current available AEB are designed to meet the requirements of collision avoidance and mitigation on dry roads although these systems show the highest benefit for accident avoidance and mitigation on slippery roads.

In this work we investigated whether the global friction potential μ_G and the wheel-individual friction potentials $\mu_{R,i}$ can be estimated during driving with an accuracy that is sufficient to adapt the intervention strategy of an AEB.

The analysis of the manoeuvre data using the ESN method gained a rough understanding on how well the friction potential μ_G can be estimated in certain situations based on the used sensory equipment. For a known tire, the accuracy of the estimate was better compared to data sets with varied tires. Situations were identified in which the sensor data was not sufficient to estimate μ_G, especially for manoeuvres with low accelerations.

Further investigations on the achievable accuracy during changes of the friction potential as well as the minimal set of sensors necessary are planned.

Nevertheless, to apply a methodology like the proposed one in a safety-critical system like an AEB, more investigation and testing under realistic driving conditions are necessary. Also, the verification of the estimate by other sensors is recommendable.

Bibliography

BREUER, J., 2009. Bewertungsverfahren von Fahrerassistenzsystemen. In: H. WINNER, S. HAKULI and G. WOLF, eds, *Handbuch Fahrerassistenzsysteme.* 1 edn. Wiesbaden: Vieweg und Teubner, pp. 55-68.

BUSCH, S., BRUNNER, H. and ZOBEL, R., 2006. Prognose des Sicherheitsgewinns unfallvermeidender Systeme. *ATZ Automobiltechnische Zeitschrift,* **108**(4), pp. 304-307.

Eichberger A, Tomasch E, Hirschberg W, Steffan H. Potentiale von Systemen der aktiven Sicherheit und Fahrerassistenz. *ATZ Automobiltechnische Zeitschrift,* **2001**-08, pp. 594-601.

HAYKIN, S., 1999. *Neural Networks: A Comprehensive Foundation.* Prentice Hall.

INTERNATIONAL ORGANIZATION FOR STANDARDIZATION (ISO), 2003. *ISO 7401:2003 Road vehicles. Lateral transient response test methods. Open-loop test methods*.

JAEGER, H. and HAAS, H., 2004. Harnessing nonlinearity: Predicting chaotic systems and saving energy in wireless communication. *Science,* **304**, pp. 78-80.

JAEGER, H., MAASS W. and PRINCIPE J. (EDS):, 2007. Special Issue Echo State Networks and Liquid State Machines. *Neural Networks,* **20**(3), pp. 287-432.

LUKOSEVICIUS, M. and JAEGER, H., 2009. Reservoir computing approaches to recurrent neural network training. *Computer Science Review,* **3**(3), pp. 127-149.

MITSCHKE, M. and WALLENTOWITZ, H., 2004. *Dynamik der Kraftfahrzeuge.* 4. edn. Springer, pp. 182-192.

NIEDERKOFLER, H., LEX, C., EICHBERGER, A. and ROJAS ROJAS, A.E., 2011. Potentialanalyse von aktiven Fahrwerks- und Antriebssystemen für die Anwendung in Fahrerassistenzsystemen in kritischen Fahrsituationen, VDI-Tagung Reifen - Fahrbahn - Fahrwerk, 25.-26.Oktober 2011, Hannover.

Deutsches Institut für Normung (DIN), 1994. *DIN 70000 - Fahrzeugdynamik und Fahrverhalten.*

RESEARCH COUNCIL FOR AUTOMOBILE REPAIRS, 2011. *RCAR Low-speed structural crash test protocol.Online available: http://www.rcar.org/Papers/Procedures/rcar_LowSpeedCrashTest2_2.pdf .Accessed on 17.12.2012*

ROSÉN, E. and SANDER, U., 2009. Pedestrian fatality risk as a function of car impact speed. *Accident Analysis and Prevention,* **41**(3), pp. 536-542.